Timbrel Domes of Guastavino: Nondestructive Assessments On A Half-Scale Model

Article *in* International Journal of Architectural Heritage · November 2008

DOI: 10.1080/15583050701661652

1 author:

Ece Erdogmus
Clemson University
135 PUBLICATIONS **1,184** CITATIONS

Timbrel domes of Guastavino:

Nondestructive Assessments on a Half-Scale Model

Ece Erdogmus, Ph.D.[1]

Abstract

The Nebraska State Capitol in Lincoln contains some of the best examples of timbrel vaults and domes utilizing the special Guastavino tile construction. A half scale model of one of the concentric timbrel domes in the Nebraska State Capitol is constructed at the Peter Kiewit Institute- Structures Laboratory of the University of Nebraska, United States of America. The experience of the construction of the *Model Dome* in itself is unique and therefore discussed in the paper. After the *Model Dome* is constructed, experimental modal analysis is utilized as a nondestructive technique for updating three-dimensional computer models for this structure. As a result of this study, a validated three-dimensional finite element model of the *Model Dome* is obtained and several inferences are made regarding the construction, modeling and dynamic testing of timbrel domes. The change in dynamic characteristics of a timbrel dome constructed with gypsum mortar due to environmental effects is also discussed.

Keywords: Masonry, timbrel domes, arches, nondestructive *in situ* testing, structural dynamics, experimental modal analysis, finite element models, model validation and updating

[1] Assistant Professor of Architectural Engineering, University of Nebraska-Lincoln, 203C Peter Kiewit Institute, 1110 South 67th St. Omaha, NE 68182. Eerdogmus@mail.unomaha.edu

1 Introduction

Timbrel vaults and domes are thin, lightweight and strong roof systems. In this unique construction style, thin clay or terracotta tiles are placed flatly, forming one or more layers and they are constructed without centering or other support. In the case of a dome, the bricks are placed in concentric rings to complete a semi-sphere. During the construction, the first layer of thin bricks or terra cotta tiles is placed without any formwork or centering, supported by the adhesion of the fast-setting mortar to the bordering walls. Besides vaulted ceilings, this technique of utilizing fast setting mortar and thin tiles is also used extensively in the construction of floor systems and staircases. If there is more than one layer of tiles, they are staggered to create an interlocking system of strong shell structure. Timbrel vaults are also referred to as *Catalan* vaults, because this construction style was first used in 14th century in Catalonia, Spain. The technique then expanded to the rest of the Mediterranean region by the 16th century, and some examples can be seen in France from early 18th century (Huerta, 2003).

This method of construction is introduced in the United States by Rafael Guastavino in late 19th- early 20th century (Nonell, 1999). There are over a thousand buildings with Guastavino domes and vaults; and some of the best examples are found in the Nebraska State Capitol in Lincoln, Nebraska, U.S. (Further history on Guastavino can be found in the Appendix). This intriguing appearance prompted a study by the author, who resides in Nebraska. A physical half-scale model (henceforth referred to as the *Model Dome*) of one of the concentric domes in the Nebraska State Capitol (Figures 1 and 2) is constructed, and is currently formed of a single layer of tiles.

The physical model is constructed to improve an experimental modal analysis- based finite element model (FEM) updating technique.

Experimental modal analysis is an effective method to extract several important physical characteristics of a structural system nondestructively, such as the mode shapes (deflected form), the natural frequencies of the modes that are excited, and the component and system stiffnesses. These characteristics can also be gathered through a three-dimensional finite element analysis, and the comparison of the experimental and analytical results can lead to a more accurate simulation of the structural behavior of the actual system. Experimental modal analysis have been used as a tool to assess existing structures by various scholars (Brownjohn 2002; Gentile *et. al.* 2004; Xia *et. al.* 2003; Catbas *et. al.* 2004; Xia *et. al.* 2004; Jaishi *et. al.* 2005; Cunha *et. al.* 2006; Atamturktur, 2006; and Boothby *et. al.* 2006); and a specific methodology for the validation of the finite element models of complex Gothic unreinforced masonry vaulted systems has been developed systems by the first author (Erdogmus, 2004; Erdogmus *et. al.* 2006, Erdogmus *et. al.* 2007). In this study, this method is extended to studies carried out on a half-scale physical model of a timbrel dome, and several inferences are made regarding the construction, modeling and dynamic testing of timbrel domes. The change in dynamic characteristics of a timbrel dome constructed with gypsum mortar due to environmental effects is also discussed.

2 Experimental Procedures

In this section, first the construction of the Model Dome is explained, followed by the material tests and modal tests conducted to determine the system characteristics of the Model Dome.

2.1 Model Dome Construction

A physical half-scale model of one of the concentric domes in the *Nebraska Capitol* is constructed by the author and her students (Figures 1 and 2). The selection of the subject dome

among numerous domes and vaults found in the *Nebraska Capitol* is due to its well-defined boundary conditions (it raises above a square room with four columns and uniform walls), its manageable size, its geometry as a semicircular dome, and its accessibility.

The *Model Dome* is designed through a detailed study of the *in situ* structure, architectural drawings, review of the pertinent literature on the timbrel vault construction techniques (Huerta, 2003; Ramage, 2004), and availability of appropriate materials. Similarities and differences between the currently available building materials and the authentic materials are carefully examined to make appropriate selections (Table 1).

Since authentic Guastavino tiles are no longer manufactured, clay face brick units are used for the *Model Dome*. The thickness is the most important dimension of the tiles for the scale model, as it will determine the thickness of the dome, and have a direct effect on the stiffness and modal behavior of the system. The clay tiles are 1.25 cm (½-inch) thick and satisfy the dimensions required for a half-scale model. It must be noted here that the *Actual Dome* has three layers of thin tiles to form the dome-webbing, and the *Model Dome* currently has only one layer, as the intension of the study is to perform experiments and analyses for single, double and triple layers of tiles, and eventually compare the system behavior. Two more layers of tiles will be added to the structure and several experiments will be carried out after each layer is laid. This paper's scope is limited to studies on the *Model Dome* with a single layer of tiles.

The side arches of the *Model Dome* are constructed from standard clay brick units. While the thickness of the side arches with a single layer of brick is not half of the thickness of the limestone arches of the *Actual Dome*, this is preferred to a double-ring arch, because multi-ring brickwork arches have inherently different performance characteristics than voussoir arches (Gilbert *et. al.* 1995). The adequacy of this smaller thickness for the side arches is checked for stability using the thrust-line analysis method (Heyman, 1995) before they are constructed

(Erdogmus *et. al.* 2006). As a result, however, it is observed that there are some differences in the dynamic structural behavior of a dome structure with thick side arches versus a dome structure with thin side arches. This discussion is presented later in the article.

Guastavino describes the cohesive construction system to be heavily dependent on material properties of the special mortar[†] used, which does not require exposure to air for its transformation or setting quality. He suggests that hydraulic lime and cement would satisfy these requirements, and for use in structural systems, any such mortar should also have high bond strength, that is equivalent to the Portland cement mortar (Guastavino, 1893). In the Catalan tradition, after the first course of tiles are laid with the fast setting mortar (plaster of Paris or gypsum mortar), the top layers are laid out with weatherproof Portland cement mortar, because the plaster itself is not weatherproof (Huerta, 2003; Ramage, 2004).

After reviewing the pertinent literature regarding the mortar characteristics for Guastavino Domes described above, the author has made the following decisions regarding the mortar selection and construction of the *Model Dome*: Plaster of Paris is used for the first layer of tiles of the *Model Dome,* due to its fast-setting quality and because it was successfully used in a similar model dome construction (Ramage, 2004). The second and third layers of the tiles will be laid out using Portland cement mortar as the existing first layer of the dome will be used as a formwork, and fast-setting mortar qualities will no longer be necessary.

Since the *Model Dome* is constructed as a stand-alone structure, while the *Actual Dome* is surrounded by the rest of the building extending on all four sides, the buttressing of the *Model*

[†] Note: Some scholars disagree with this argument (Saliklis *et. al.* , 2003) suggesting that the uniqueness of this construction does not come from the mortar's characteristics. The author of this study initially stands neutral to this debate. However it is evident from the construction experience gathered in this study that, while the strength characteristics of the mortar may not affect the dome's structural behavior substantially, the fast-setting characteristics are certainly important for the no-formwork or no-centering construction style. This has been proved by the construction experience differences between the side arches (clay units and conventional Portland cement lime mortar) and the dome (clay units and Plaster of Paris).

Dome's base is an important consideration. It is impossible to create the exact boundary conditions and the overall lateral deflections of the *Actual Dome* for modal behavior, but attention is given to the supports to make sure that the thrusts[‡] from the arches and the dome are restrained and there are no failures due to support instability during the construction or after, which is known as one of the most common reasons behind the failure of arch-type structures (Ochsendorf, 2002). Therefore, four masonry piers at the corners and a timber base frame are constructed to provide restraints (Figure 2).

Timbrel dome construction style is unique, therefore, for this project, first the style as described in the literature is carefully studied (Guastavino, 1893; Ramage, 2004; Huerta, 2003), and then constructed as follows:

First the side arches are constructed out of standard clay bricks and Type N, Portland cement lime (PCL) mortar (Table 1), in the conventional masonry arch building style using a custom made centering (Figure 3). Once the four side arches are built and cured, the tile dome is constructed without formwork or centering, to mimic the authentic construction style of timbrel vaults. In the construction of the *Model Dome,* the center of the structure is found by running two string lines between the four abutting piers in the shape of a letter "X" (Figure 4). A string line is fixed to the base of the structure at the center in order to set the height corresponding to the springing point of the arches, which is ten inches above the ground surface. From this point, a length of string line equivalent to the radius of the dome is used to set the individual tiles one by one at a common radius. With each tile set equidistant from a common center, the structure assumes the perfect form of a spherical dome. This style of construction developed for this study

[‡] Once again, there are opposing claims regarding whether or not the timbrel domes exert thrusts. The author currently does not support either of these opinions as she wishes to first conclude her research on the matter and find scientific evidence. However, *if* the dome does exert thrusts, as suggested by some scholars (Huerta, 2003), as opposed to Guastavino's claims (Guastavino, 1893); the timber framing provided *would* resist these thrusts along with the thrusts from the side arches.

resembles one of the historical methods of construction for timbrel domes as illustrated in Huerta (2003), where a rod attached to a fixed point is used to control the geometry when building a dome without formwork or centering.

2.2 Laboratory Testing for the Material Properties of the Model Dome

The material properties necessary for a linearly elastic solid model are density (d), modulus of elasticity (E_m), and Poisson's ratio (v). It is also important to also gather the compressive strength (f'_m) value for future nonlinear analyses, or to gather E_m values. An initial range of material properties are gathered through sample testing in the laboratory (Table 2) in order to increase the accuracy of the parameter extraction and model updating procedures.

Five masonry prisms for the regular clay brick and mortar assembly (Material Set 1), and three prisms for the thin clay tile and plaster of Paris assembly (Material Set 2) are built with the same workmanship that was used for the construction of the *Model Dome*. After the specimens cured for twenty-eight days, they are tested for compressive strength (f'_m), modulus of elasticity (E_m) and Poisson's ratio (v). Testing is performed in accordance with ASTM C1314-03b (ASTM, 2005) at the Structures Laboratory of the University of Nebraska. Using the results of these experiments, arrays of values for each material property are gathered, providing initial values for the finite element models of the *Model Dome.*

Strain gages applied to the masonry prisms are used to measure longitudinal and transverse strain, and the load is incrementally increased and recorded to gather stress values. Test data is analyzed, revealing the ranges of compressive strength, modulus of elasticity and Poisson's ratio values for the two types of masonry construction. After the test data is analyzed, it is discovered that the ultimate compressive strength results from these tests are more consistent than those for the strain gage data, therefore the general relationship given in the Masonry

Standards Joint Committee 2005 Code and Specifications (MSJC 2005), linking the assembly compressive strength (f'_m) and the modulus of elasticity is used to estimate an initial range for the assembly modulus of elasticity (E_m) in this study ($E_m = 700f'_m$). Using this relationship, a range of values for E_m are determined for material sets 1 and 2. These ranges of values are listed in Table 2.

Poisson's ratio values are gathered from the ratio of the longitudinal-to-transverse strain data gathered from the strain gages. The average values of Poisson's ratio are 0.24 and 0.20 for the standard brick and the face brick, respectively. The density values of the materials are determined by the buoyancy tests conducted for the clay brick and thin clay tiles. The average density value for the former is 2,300 kg/m^3 (0.0026 slug/ in^3) and for the latter it is 1,800 kg/m^3 (0.0020 slug/ in^3).

Based on initial analyses and sensitivity studies, which will be explained in Section 3, the average values for the density and Poisson's ratio are directly used in the computer models, while a fine tuning of E_m values along with boundary conditions is carried out through comparisons with experimental results.

2.3 Dynamic Experiments on the Model Dome for FEM Validation

Several dynamic modes of the *Model Dome* are observed when small force, low frequency excitations are applied to the structure with an instrumented hammer (PCB Piezetronics ICP® Impulse Hammer Model 086D20). The force sensor in the hammer measures the load input, and the vibrations generated in the structure are measured using seismic shear accelerometers (PCB Piezotronics model 393A03 seismic accelerometer with a sensitivity of 1V/g). Two dynamic signal analyzers are used interchangeably in this study: SIGLAB® and Dactron Photon II®. These two systems have similar characteristics and they generate results that

are in agreement; thus the results presented in this paper are not differentiated according to the signal analyzer. After the test data is gathered, the acceleration *frequency response function* (FRF) is plotted, which is a ratio of the acceleration response to the transform of the driving force. From the FRF functions, several system characteristics are extracted and used in the finite element model updating and validation.

Modal testing can be employed in two different ways: Fixed excitation and fixed response modal testing. Fixed response method is used for the dynamic experiments on the *Model Dome*. In this setup, a single accelerometer is located at a pre-determined position and the hammer impact is applied at several points on the structure. This method requires two input channels on the signal analyzer (one for the accelerometer and one for the hammer), and it is useful in applications where a single-unit signal analyzer is used or when experiments are conducted at remote locations. Each test is repeated 3 to 5 times to assure data quality, which is checked by plotting the coherence (COH) function. A definition of the COH function can be found in Ewins (2000). Coherence function approaching unity indicates a linear trend between the output and input, and in most cases represents high confidence in the measured data (Ewins, 2000; Hanagan *et al.*, 2003).

Using the modal analysis tools for post-processing, measurements from all of the points can be combined to display the observed mode shapes on a user created geometric model of the structure (Figure 5), and to list the natural frequency values for the observed modes. The accuracy of the estimated mode shape increases as the number of data points tested increases. The geometric model of the *Model Dome* comprises of 65 points, however, as confirmed by experiments, the points around the supports do not move. Therefore, only 48 of the 65 points are actual data points.

Two sets of experiments are performed: Setup #1, where a single accelerometer is located at the quarter point of one of the quadrants (point 51, Figure 5a); and Setup #2, where a single accelerometer is located at the crown (point 1, Figure 5b). In both tests, a hammer impact is applied at each of the 48 points. First three modes observed in Setup #1 all have frequencies smaller than the first mode observed in Setup #2. The natural frequencies of these first three modes are 43.5, 50.6, and 86.7 Hz (Figure 6a). Setup #2 results in the observation of modes that are mostly in the higher frequency range. The first mode that can be observed with this setup has a natural frequency of 96.8 Hz (Figure 6b). This is mainly because the crown, where the sensor is located at this setup is a node for various modes observed in Setup #1. A node is defined as a point with no substantial displacements for the mode that is being observed.

As can be seen, in order to thoroughly study the modal behavior of a complex structure, various points must be tested. Since there are numerous combinations of experimental setups that can be performed, studying the modal behavior of the structure on a preliminary analytical model, and planning the testing setup is very beneficial. The test setups in this study are the results of such a preliminary analysis.

3 Updating of the FEM and Dynamic Characteristics

In this study, three-dimensional models of timbrel domes are created and updated using experimental modal analysis. The iterative methodology employed in this study is presented in Figure 7. After the models are created; initial boundary conditions and average material properties are entered, appropriate element types are selected, sensitivity analyses are performed, and the experimental setup is designed through preliminary analyses. Once the dynamic experiments are carried out on the *Model Dome*, the experimental results are compared to analytical results until an optimum agreement for mode shapes, natural frequencies, and component stiffness is achieved. It must be noted here that while this iterative process takes

place, the material properties are only varied within the initially established range (Step 3 in Figure 7, Table 2).

Upon application of the steps 1-4 (Figure 7) on the *Model Dome*, sensitivity analyses are carried out to establish the influence of each of the material properties on the resulting dynamic behavior. A more detailed explanation on how sensitivity analyses are performed on the complex masonry structures using finite element models can be found in Erdogmus (2004), while broader explanations of the topic can be found in the text by Ewins (2000). The results of the sensitivity analyses are presented in Table 3, and the following conclusions can be drawn from these results:

1. It is seen that the mode shapes are mainly affected by the geometry of the structure and the boundary conditions. However, along with this conclusion some assumptions and observations must be noted. A simplifying assumption of the uniform distribution of mass (homogenous material) is adopted such that the masonry-mortar characteristics are represented as the effective characteristics of a masonry assembly. Moreover, the component stiffnesses and the distribution of stiffness within the structure are also found influential in the modal behavior.
2. The sensitivity analyses suggest the effect of the three elastic material properties to rank as follows: 1) Modulus of elasticity, 2) density, and 3) Poisson's ratio, for both material sets. These results from the sensitivity analyses are as anticipated by the author based on fundamental theories of structural vibrations and engineering judgment. The stiffness and mass both play important roles in a system's modal behavior, as the former is directly, and the latter is inversely proportional to the natural frequency. Among the two, E_m values directly affect the stiffness of the system in dynamic behavior, while the mass depends also heavily on the size of the system.

3. With two separate sets of material properties defined for the side arches and the dome-webbing, changes in the values assigned in each one of these sets affect different dynamic modes of the system, and at varying levels.

3.1 Finite Element Model Creation

FEMs for this study are created using the finite element software ANSYS. The models are assumed to behave linearly elastic, since such an assumption is proved to be appropriate within the range of the dynamic loads applied during the experiments (Erdogmus, 2004). In all of the models used in this study, three-dimensional arches and the corner piers are created as solid volumes and are meshed with SOLID45 elements. To model the dome-webbing, however, two types of models are created: 1) SHELL dome model (Figure 8a): The dome-webbing is modeled as a two-dimensional curved surface and it is meshed with SHELL63 elements. The thickness of the webbing is entered as a property of the shell element. 2) SOLID dome model (Figure 8b): The dome-webbing is modeled as a volume and it is meshed with SOLID45 elements.

While the analytical results for these two models are discussed later in the article, the characteristics of SOLID45 and SHELL63 elements are briefly explained here.

SOLID45 is defined by eight nodes and the orthotropic material properties. Each of the eight nodes has three degrees of freedom: translations in the nodal x, y, and z directions. The element has plasticity, creep, swelling, stress stiffening, large deflection, and large strain capabilities. In the case of the "SHELL dome models" created in this study, the dome-webbings are modeled using shell elements (SHELL63), and the thickness is entered as a parameter (based on the real dome thickness), so that a surface actually represents a volume. SHELL63, which is defined as elastic shell, has both bending and membrane capabilities. Both in-plane and normal loads are permitted. The element has six degrees of freedom at each node: translations in the

nodal x, y, and z directions and rotations about the nodal x, y, and z-axes. Stress stiffening and large deflection capabilities are included. A consistent tangent stiffness matrix option is available for use in large deflection (finite rotation) analyses (ANSYS 2007).

3.2 Validation of the FEM and Dynamic Characteristics

Once the experimental results and the analytical models are both available, the analytical models are updated using the methodology presented in Figure 7. The results of the application of this procedure to the *Model Dome* are presented in the next sections.

3.2.1 Boundary Condition Validation through a Comparison of the Mode Shapes

The boundary conditions of the structure are very straight forward, as the *Model Dome* is created in controlled lab conditions, and the entire structure is simulated with the FEM. These boundary conditions are such that the base of each pier (*i.e.* all 4 support points) is restricted against lateral translation and vertical movement, along with rotations around the three axes. These boundary condition assumptions match well with the actual structure that is constrained at the supports in all degrees of freedom (Figures 1 and 2). No other constraints are applied to the model.

The first set of experiments on the *Model Dome* is conducted soon after the completion of construction and it is used to update the FEM of the undamaged/ initial structure. A comparison of experimental and analytical deformed shapes for the 1st mode is given in Figure 9. Both mode shapes show a bending deformation and maximum vertical displacements at the quarter points of the side arches and the dome. Deformed shapes of the modes 2-4 are illustrated in Figure 10, and the descriptions of the mode shapes are listed in Table 4. All of the experimentally observed

modes present closely matching deformed shapes with the analytical results. The agreement of mode shapes provides a validation of the assumed boundary conditions.

As mentioned before, the side arches of the *Model Dome* are less than half of the thickness of the limestone arches of the *Actual Dome*. While the thinner side arches have proven to be perfectly functional and stable, it is possible that there are substantial differences between the dynamic behavior of a dome with thick side arches versus a dome with thin side arches. In order to evaluate this hypothesis, a dome model with thick side arches is created (Figure 8c). When the mode shapes generated by the *hypothetical thick side arch model* (Figure 8c) are inspected, it is seen that in lower frequency modes the dome-webbing engages in isolated motion from the supporting side arches. However, for the original *Model Dome* models, even the most dominant crown motion involves some motion of the side arches. This contrast in modal behavior is because when the side arches are thicker, *i.e.* stiffer, a larger difference between the component stiffnesses of the side arches and the dome-webbing occurs. As a result, the side arches of the *hypothetical thick side arch model* act as stiff supports for the relatively more flexible dome and causes substantial movements in the dome-webbing (specifically the crown) in lower frequency modes, which is not observed until the 6^{th} or the 9^{th} modes for the original *Model Dome*. This brief analysis also makes it clear that the mode shapes are strongly influenced by the distribution of stiffness within the structure.

3.2.2 Material Property Validation through a Comparison of the Natural frequencies

Once the corresponding analytical and experimental modes are determined, the natural frequencies for these modes are compared between the analytical and experimental values. This part of the procedure provides a validation for the initially entered modulus of elasticity (E_m); density (*d);* and the Poisson's ratio (ν) values. As mentioned before, based on the sensitivity analyses carried out, among the three material properties, E_m is found to have the largest

influence on the dynamic behavior of the system. For this reason, the averages of the experimentally obtained values for the *d* and *v* values are used directly, while the E_m values are varied within the previously established range of values until a reasonable agreement is reached between the analytical and experimental natural frequency values (Table 4). When this procedure is applied to the *Model Dome*, the final material properties listed in Table 5 are achieved. The closely matching mode shapes and natural frequencies with 2.3-3.9% error for the first mode comparison, and a maximum error of 10% overall, present a good agreement between experimental and analytical results (Table 4).

3.2.3 Component Stiffness Approximation

The displacement FRF at zero frequency yields the inverse of the stiffness of the structural component that is tested (k_s) or the flexibility ($f_s=1/k_s$). This information can also be gathered from the analytical model by finding the displacement per unit force through a static analysis, at a point where the excitation and the response is measured experimentally (Step 11 in Figure 7). Thus, the comparison of the experimental and analytical values provide the last step of the model updating technique.

In theory, a displacement function can be gathered from the acceleration data, and the component stiffness (k_s) can be determined from the reciprocal of the zero frequency point on the displacement FRF function plot. This method is very promising in terms of validating the analytical models for stiffness, however in practice there are problems, since the experimental data is recorded in terms of acceleration and it is necessary to convert it to displacements. Ambient noise results in very small vibration amplitudes at the lower frequencies, and the displacement plot at these lower frequencies becomes unreliable. Nevertheless, if the displacement FRF for a simple system (such as a single degree of freedom system) is inspected,

it is observed that the plateau starting at the root of the resonant peak can be extrapolated to 0-Hz and an approximation for the component stiffness is possible. Using a similar simplification, the system stiffness values gathered experimentally and analytically can be compared (Figure 11 and Table 6).

As can be seen, while the values are in the same order of magnitude, there is a large discrepancy. This is mainly due to the fact that, while the idea is very promising, it is currently a very rough estimation. The author has ongoing research on this topic and some of the current findings are discussed in Section 3.3.

3.2.4 Comments Regarding Element Type Selection

In order to decide the most appropriate model among the alternatives, the characteristics of the element types are examined, the pertinent literature is reviewed, and modal analyses are carried out. As a result, SOLID Dome models are selected to be the more viable option for the following reasons:

1) While both models provide a good correlation in general for mode shapes and their respective natural frequencies, the SOLID model presents a much better correlation with experimental results in terms of the system stiffness approximation (Tables 4 and 5).
2) When the solid and shell elements are simultaneously used in a model, a compatibility problem occurs at the junction of areas with these different elements. Modeling the dome-webbing with solid elements solves this problem.
3) Atamturktur (2006) has carried out a continuation of the author's doctorate work and compares the author's initial selection of shell elements (SHELL63) to SHELL93 elements. Noting a better correlation in mode shapes for the axisymmetric modes,

Atamturktur recommends use of SHELL93 elements. While this recommendation has merits for further investigation, with the selection of SHELL93 elements, the problems with solid-shell element compatibility and the incorrect estimates of the dome stiffness should also be addressed. Nevertheless, the problems listed by Atamturktur are taken into consideration and thus considered as further motivation to prefer solid elements.

3.3 Further dynamic experiments on the Model dome

The author believes that the relative stiffnesses of the structural components are important characteristics that can be gathered from modal testing and further development of this section of the model validation technique for complex systems has strong merits. Thus, one of the goals of this ongoing study is to improve this portion of the method by investigating alternative ways of measuring stiffness nondestructively. Several experiments are conducted throughout a calendar year, and the results are summarized in this section.

3.3.1 Results of the second set of experiments

Keeping the testing methodology and the test points constant, a second set of modal experiments is carried out six months after the first set, and during this period the *Model Dome* was outside, covered by a plastic tarp, enduring a Nebraska summer. Summers in Nebraska are usually dry and extreme temperatures as high as 38-40 ℃ (+100 ℉) are observed. It is possible that there has been a substantial loss of water in the fast-setting mortar. The measured natural frequency for the first observed mode in this test is 51.5 Hz, an 18% increase over the first set of experimental values. This increase in the natural frequency may be the result of drying plaster of Paris. As the plaster dries, it loses its softness and flexibility and substantial shrinkage cracking occurs when constrained by the clay brick units. During the second set of testing, cracks and lost

mortar are observed on the dome, supporting this thesis. Moreover, loss of water, falling of dried mortar, and cracks all mean a decrease in structural mass. The loss of flexibility (increasing stiffness) and reduced mass results in an increased natural frequency, when the basic relationship between natural frequency, stiffness and mass is considered: $\omega = \sqrt{k/m}$, where, ω is the natural circular frequency, k is the system stiffness, and m is the system mass.

Another important discussion here is that, while the initially created structure is tested in its linear range using the hammer impacts, the second set of experiments are made on an already cracked structure, even though the cracks are due to environmental conditions and not increased loading. This condition creates a good analogy to the assessments and model updating that are carried out on real structures, where adjustments on material properties must be made based on the age and the actual condition of the structure. Moreover, if the behavior of the cracked structure under external load cases are to be studied after this point (earthquake, wind, etc…), a nonlinear FEM must be created.

3.3.2 Results of Dynamic experiments with added mass

According to the basic equation given in the previous section, which assumes undamped, forced vibrations in the linear range of the material, an increase in the mass of the structure results in a decreased natural frequency when the stiffness, boundary conditions, and geometry is constant. The mass of the *Model Dome* is 4630 kg as calculated using the dimensions and densities of the finite element model. An extra mass of 45 kg is applied to the dome in the form of a point load placed at the crown, and the modal experiments are repeated. Starting with the natural frequency of 51.5 Hz measured the same day, the anticipated decrease is very small, around 0.2 Hz, resulting in an estimated natural frequency of 51.3 Hz. The measured frequency during this experiment is 51 Hz, which presents a decrease of 0.5 Hz instead of 0.2 Hz. The

error is small at 0.5% and can probably be eliminated if a larger mass difference between the dome's total mass and the additional mass is employed. The small change in the total mass (0.09%) is not enough to observe substantial changes or to extract accurate stiffness information from the experiment. The decreasing natural frequency, however, provides more evidence for the suitability of the simplifying assumption of the linear relationship assumed. This preliminary attempt also illustrates the potential of a methodology where the stiffness is kept constant and the total mass is increased substantially to more closely estimate the system stiffness of a complex structure using nondestructive testing methods.

4 Conclusions

Several conclusions can be drawn from this study:

1. A half-scale physical model of a concentric timbrel dome at the Nebraska State Capitol is successfully constructed. No centering or formwork is used during the construction of the semi-spherical dome construction. The construction experience is worthwhile to understand the unique Guastavino construction technique. It is found out that the fast-setting mortar is important for the construction of timbrel domes, especially the first layer of tiles. Additional layers of tiles can be laid with any mortar of choice, since the first layer will provide a formwork and support. The *Model Dome* is built without prior mason skills, quickly and without centering, yet it is very strong and durable.

2. *Model Dome* analytical model is successfully updated such that the final material properties are within the pre-established range of values from laboratory testing of the construction materials and optimal agreement with modal experiment results are obtained.

3. Sensitivity analyses for the material properties reveal the effect of each modeling parameter on the resulting structural dynamic behavior. The mode shapes are mainly affected by the geometry of the structure and the boundary conditions. However, along with this conclusion some

assumptions and observations must be noted. A simplifying assumption of the uniform distribution of mass (homogenous material) is adopted such that the masonry-mortar characteristics are represented as the effective characteristics of a masonry assembly. Moreover, the component stiffnesses and the distribution of stiffness within the structure are also found influential in the modal behavior. It is also noted that with two separate sets of material properties defined for the side arches and the dome-webbing, changes in the values assigned in each one of these sets affect different dynamic modes of the system, and at varying levels.

Finally, the sensitivity analyses suggest the effect of the three elastic material properties to rank as follows: 1) Modulus of elasticity, 2) density, and 3) Poisson's ratio, for both material sets. These results from the sensitivity analyses confirm the expectations of the author based on engineering judgment.

4. It is concluded that modeling the dome-webbing as a curved surface and using shell elements may present problems, and models with solid elements are recommended.

5. In order to evaluate the hypothesis that the *Model Dome* with its thinner side arches would present a different modal behavior than the Actual Dome, a dome model with thick side arches were created. When the mode shapes generated by this *hypothetical thick side arch model* were inspected, it was seen that in lower frequency modes the dome-webbing engages in isolated motion from the supporting side arches. However, for the original *Model Dome* models, even the most dominant crown motion involves some motion of the side arches. This brief analysis makes it clear that the mode shapes are strongly influenced by the distribution of stiffness within the structure. These findings will prove very useful when comparisons to the Actual Dome are made in the future work.

6. Further experiments carried out on the *Model Dome* suggest that this technique may provide a means to nondestructively assess structural component stiffness. Over time, masonry structures

may experience a loss of flexibility and mass due to migration of water from mortars. This loss of flexibility and mass will increase the natural frequency of the structure. Conversely, an increased structural mass should result in a decreased natural frequency for the structure. A preliminary investigation shows that this conjecture seems to hold true, however, the additional mass was small relative to the mass of the structure. The results of these experiments provide evidence to support the assumption of linear structural behavior within the range of dynamic loads applied. Future work will include increasing the additional mass in an attempt to accurately determine the system stiffness.

5 Acknowledgements

The author wishes to extend her gratitude to Thomas Kaspar, Robert Ripley, Michael Rindone, and Karen Wagner of the Nebraska State Capitol for providing access to the building and the archives, and for sharing their knowledge on the building's design and construction history. The materials for the dome are donated by The Brick and Stone Store, Lumberman's, and Rinker Materials. Their generosity is deeply appreciated. The artists who have created the *Model Dome* under the supervision of the author are three outstanding students of the University of Nebraska- Architectural Engineering Program: Brian Skourup, Matthew Radik and Neel Keiser. Without their dedication and talent, this study would simply not be possible. The author also acknowledges Matthew Radik's contributions in the creation of the computer models, and Brian Skourup's assistance in analyses and editing. Last but not the least, the author presents her gratitude to the editors and the reviewers for providing very helpful comments and suggestions.

6 References

ANSYS (2007). *ANSYS Elements Reference.* ANSYS Release 10.0.

ASTM C1314-03b (2005). "Standard Test Method for Compressive Strength of Masonry Prisms," ASTM.

Atamturktur, H.S. (2006) *Structural Assessment of Guastavino Domes.* Masters Thesis. The Pennsylvania State University, May 2006.

Boothby, T.E, Atamturktur, H.S., Hanagan, L.M. (2006). "Modal Analysis Methods for Validation of Vaulted Stone Masonry Models", *Proceedings of the 2006 Architectural Engineering Conference, ASCE.*

Brownjohn , J.M.W. (2002). "Ambient vibration studies for system identification of tall buildings,"*Earthquake Engineering and Structural Dynamics*, v 32, n 1, January, 2003, p 71-95.

Catbas, F. N.; Brown, D. L.; Aktan, A. E. (2004). "Parameter estimation for multiple-input multiple-output modal analysis of large structures," *Journal of Engineering Mechanics*, v130, n 8, August, 2004, p 921-930.

Cunha, A., Caetano, E. (2006). "Experimental modal analysis of civil engineering structures,"*Sound and Vibration*, v 40, n 6, June, 2006, p 12-20.

Erdogmus, E. and Skourup, B. (2007). "System Characteristic Identification of Timbrel Domes Using Modal Analysis," *2nd International Operational Modal Analysis Conference*, Copenhagen, Denmark, April 30th-May 2nd 2007.

Erdogmus, E. and Skourup, B. (2006). "Experiments and Analyses on a Timbrel Dome," *Proceedings of the 2006 Architectural Engineering Conference, ASCE.*

Erdogmus, E. (2004) "Structural Appraisal of the Florentine Gothic Construction System". *Ph.D. Thesis*. The Pennsylvania State University, August 2004.

Ewins, D. J. (2000). *Modal testing: theory, practice, and application*. Baldock, Hertfordshire, England; Philadelphia, PA: Research Studies Press.

Gentile, C. and Martinez y Cabrera, F. (2004). "Dynamic performance of twin curved cable-stayed bridges," *Earthquake Engineering and Structural Dynamics*, v 33, n 1, January, 2004, p 15-34 .

Gilbert, M., Melbourne, C. (1995). "Analysis of multi-ring brickwork arch bridges," in *Arch Bridges*, Ed. Melbourne, C., 1995.

Guastavino, R. (1893). *Essay on the Theory and History of Cohesive Construction, Applied Especially to the Timbrel Vault.* Ticknor and Company, Boston.

Hanagan, L.M., Raebel, C.H., and Trethewey, M.W. (2003) "Dynamic Measurements of In-Place Steel Floors to Assess Vibration Performance." *Journal of Performance of Constructed Facilities, ASCE*, 17(3), 126-135.

Heyman, J. (1995). *The Stone Skeleton*. Cambridge University Press.

Huerta, S. (2003). "The Mechanics of Timbrel Vaults: A historical Outline," from the book titled *Essays on the History of Mechanics*, edited by Becchi, A., Corradi, M. Foce, F. and Pedemonte, O., Birkhäuser Verlag, Berlin.

Jaishi, Bijaya, Ren, Wei-Xin (2005). "Structural finite element model updating using ambient vibration test results," *Journal of Structural Engineering*, v 131, n 4, April, 2005, p 617-628.

MSJC (2005). *Masonry Standards Joint Committee (MSJC) Building Code Requirements for Masonry Structures (ACI 530/ASCE 5/TMS 402 and ACI 530.1/ ASCE 6/TMS 602), and Specification for Masonry Structures (ACI 530/ASCE 5/TMS 402 and ACI 530.1/ASCE 6/TMS 602).*

McKee, J. (2004). "Guastavino tiles lend strength, beauty to ceilings at Capitol," *Lincoln Journal Star*, Lincoln, Nebraska. (Sunday, September 26, 2004).

NE Capitol Archives (2004). *Personal notes of Erdogmus, E.* (September 29, 2004).

Nonell, J. (1999) "La obra arquitectonica de Rafael Guastavino en Cataluna." *Las bovedas de Guastavino en America*. Instituto Juan de Herrera. Madrid, Spain.

Ochsendorf, J.A. (2002). *Collapse of Masonry Structures.* PhD Thesis, University of Cambridge.

Ramage, M. (2004). http://architecture.mit.edu/class/guastavino/main.htm

Parks, J. And Neumann, A. G. (Eds.) (1996). *The Old world builds the New: The Guastavino Company and the technology of the catalan vault, 1885-1962.* Exhibit Catalogue. New York: Avery Architectural Library and the Miriam and Ira D. Wallach Art Gallery, Columbia University.

Saliklis, E. P., Kurtz, S.J., Furnbach, S.V. (2003). "Finite element modeling of Guastavino tiled arches," *Proceedings of the Eighth International Conference on Structural Studies, Repairs and Maintenance of Heritage Architecture,* May 7-9 2003 Halkidiki, Greece.

Thompson, E. (2004). *The Soundscape of Modernity : Architectural Acoustics and the Culture of Listening in America, 1900-1933.* The MIT Press; New Ed edition (October 1, 2004).

Xia, Pin-Qi, Brownjohn, J. M. W. (2004). "Load-carrying capacity evaluation of damaged reinforced concrete structures by dynamic testing and finite-element model updating," *Journal of Testing and Evaluation*, v 32, n 5, September, 2004, p 366-372

Xia, Pin-Qi, Brownjohn, J. M. W. (2003). "Residual stiffness assessment of structurally failed reinforced concrete structure by dynamic testing and finite element model updating,"*Experimental Mechanics*, v 43, n 4, December, 2003, p 372-378.

7 Appendix: Brief History on Guastavino in the U.S.

Rafael Guastavino was born in Valencia, Spain in 1842. He studied architecture and began designing homes in 1866. While continuing his architecture practice in Barcelona, he got interested in the construction of timbrel vaulting. During the U.S. centennial, he submitted an

entry to the Philadelphia exposition, and won a design medal. Then, in 1881, he immigrated to the U.S. (Woburn, Massachusetts) together with his nine year old son, Rafael Junior. His interest in timbrel vaulting system continued and, in 1893, he wrote a book on the topic (Mckee, 2004; Guastavino, 1893). Some of his achievements in tile manufacturing and construction were awarded patents. He took the established Catalan vaulting principles and used them to design arches, domes, vaults and staircases in numerous important buildings in the U.S.

In 1907, Guastavino, together with his son, started the Guastavino Fireproof Construction Company (no more extant), with offices in Woburn, MA and New York. Their innovative, patented tiles were custom-designed and manufactured for vaults, staircases, domes, arches, and other architectural features (Parks and Neumann, 1996). They then designed and constructed the Basilica of St. Lawrence at Asheville, North Carolina. The most significant feature of the building was the central ceiling, which, at 18 by 25 meter (58 by 82 feet), was the largest free-standing elliptical dome in North America, at the time. Construction of the basilica began in 1905 and was completed in 1909 by Rafael Guastavino, Jr. after his father died in 1908. The senior Guastavino is interred in a niche in the church. In 1914, the company introduced special acoustical tiles, called Akoustolith, through collaboration with Wallace Sabine at Harvard. Thus, the company became renowned not only for its fireproof (*Rumford*) tiles, but also for the akoustolith tiles, which have rougher and more porous surfaces for improved sound absorption properties (*NE Capitol Archives; Thompson, 2004*).

Father and son Guastavino together created the most distinctive features of nearly one thousand buildings in North America. A few of the notable buildings in the U.S. with Guastavino features include the Boston Public Library, the U.S. Army War College in Washington, D.C., the Federal Reserve Bank of New York, and the subject of this paper, the Nebraska State Capitol Building (henceforth referred to as the *Nebraska Capitol*).

When New York architect Bertram Goodhue won the design competition for the new *Nebraska Capitol* in 1920, one of the materials he specified was the Guastavino tile, which he considered to be very unique and crucial to his concepts. As a result, the *Nebraska Capitol* includes numerous examples of Guastavino work, including examples of polychromatic or monochromatic tiled vaults and domes, walls of some of the meeting rooms constructed with akoustolith tiles, and even the special acoustic Guastavino plaster used as the finish for the ceilings of the library. It seems like the only Guastavino feature that is not found in the *Nebraska Capitol* is an example of the tile staircase.

McKee (2004) refers to the strength of Guastavino's vaulted ceilings as follows: "a ceiling so strong [that] even a good-sized hole would not significantly alter the strength of the arch". This claim may sound exaggerated and unrealistic for masonry vaults; however, there are evidences in the *Nebraska Capitol*, where the vaults, arches and domes support substantial point loads from the roofs through columns. This observation aggravates the debate of whether or not timbrel vaults and domes are substantially different than regular masonry, because it can be argued that a regular masonry vault, dome or arch would not be used to support point loads. The good condition of these load bearing domes and vaults, however, support the claims of some scholars, who, along with Guastavino himself, have great confidence in the capabilities of these structural systems. Therefore, the question remains: Should a timbrel vault or dome be considered as ordinary masonry construction, or should it be considered as a unique type of thin-shelled structure? This study makes a step towards answering this question by providing validated computer models and some input regarding the structural behavior of these systems, yet a solid answer for such a highly debated question can only be gathered through a more in-depth study that is beyond the scope of what is presented in this article.

Figure Captions

Figure 1. The concentric Guastavino tile timbrel dome located in the Nebraska State Capitol that is studied in the project.

Figure 2. *Model Dome* constructed at the Peter Kiewit Institute Structures Laboratory of University of Nebraska

Figure 3. Construction of the Side arches with centering. Two centering pieces are constructed, therefore two side arches are built simultaneously. The centering is removed after the arch cures for a day, then it is re-used.

Figure 4. Construction of the Model Dome. The strings tied to the springing of arches are crossed at the center of the sphere, and a radius-length string is used to locate each tile equidistant from the center, thus forming the semi-spherical dome shape.

Figure 5. Experimental setups for the *Model Dome* shown on a 65-point geometric dome model created in STARMODAL

Figure 6. Experimental results for the *Model Dome* shown on a 65-point geometric dome model created in STARMODAL

Figure 7. Summary of Experimental Modal Analysis Based FEM Updating Methodology

Figure 8. Analytical Models for the *Model Dome*

Figure 9. Comparison of experimental and analytical mode shapes for Mode #1

Figure 10. Analytical mode shapes for the SOLID model

Figure 11. Frequency Response Function Displacement Magnitude Plot for one of the experiments conducted for the *Model Dome* and the comparison to the analytical approximation

Table Captions

Table 1. Model Dome Components and Materials

Table 2. Initial Material Property Ranges for *Model Dome* based on Laboratory Testing

Table 3. *Model Dome* Finite Element Models- Parametric Sensitivity Analysis Results

Table 4. Experimental results for the Model Dome for Natural Frequency Validation

Table 5. Final Material Properties for the *Model Dome* Finite Element Models

Table 6. Experimental Results for the Model Dome for Stiffness Validation

Figure 1. The concentric Guastavino tile timbrel dome located in the Nebraska State Capitol that is studied in the project.

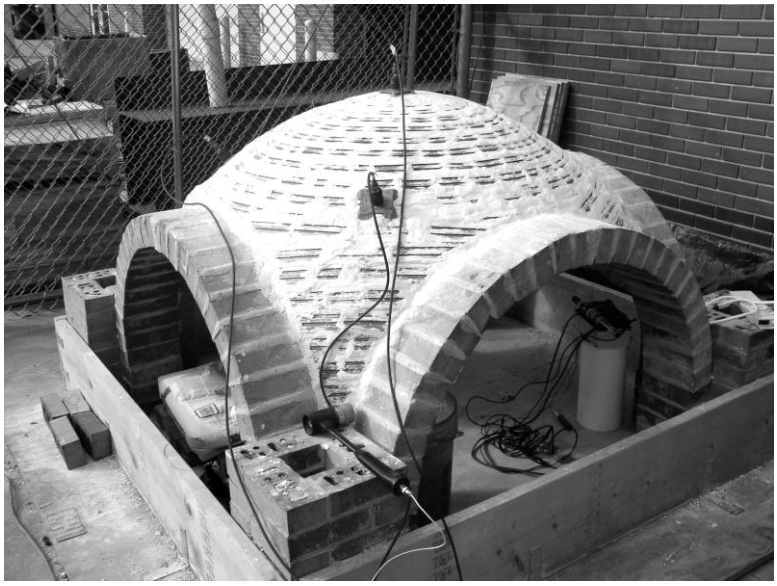

Figure 2. ***Model Dome*** **constructed at the Peter Kiewit Institute Structures Laboratory of University of Nebraska**

Figure 3. Construction of the Side arches with centering. Two centering pieces are constructed, therefore two side arches are built simultaneously. The centering is removed after the arch cures for a day, then it is re-used.

Figure 4. Construction of the Model Dome. The strings tied to the springing of arches are crossed at the center of the sphere, and a radius-length string is used to locate each tile equidistant from the center, thus forming the semi-spherical dome shape.

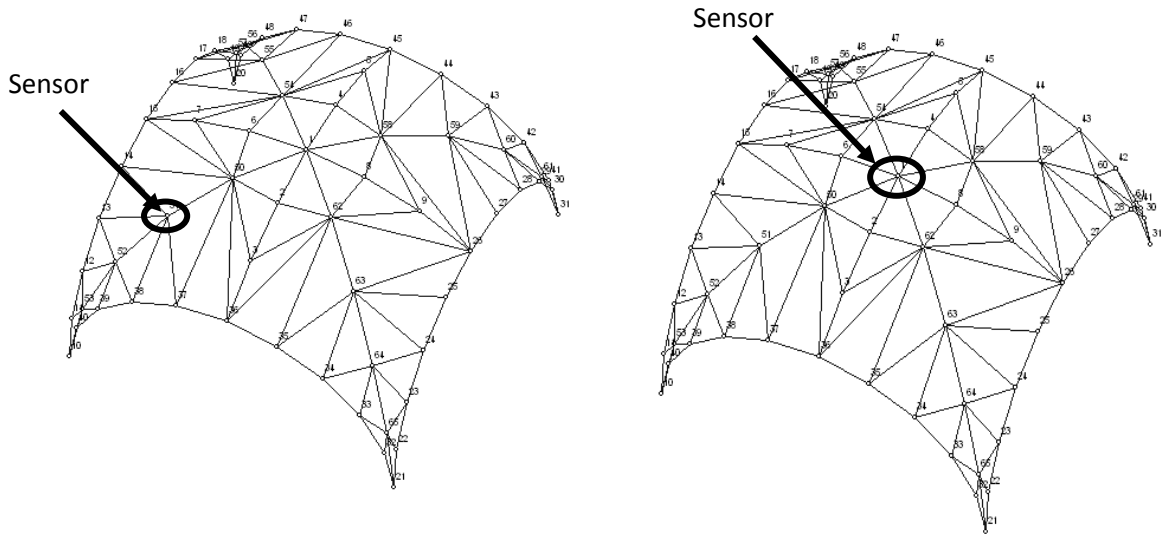

a) Setup #1 b) Setup #2

Figure 5. Experimental setups for the *Model Dome* shown on a 65-point geometric dome model created in STARMODAL

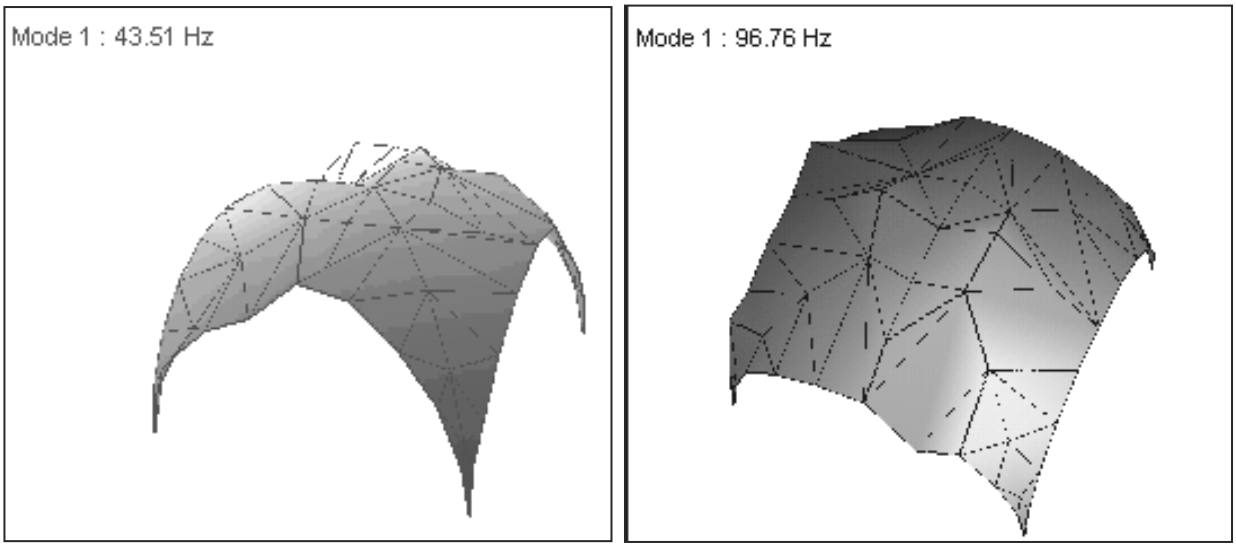

a) Setup #1: First observed mode at 43. 51 Hz.

b) Setup #2: First observed mode at 96.8 Hz.

Figure 6. Experimental results for the *Model Dome* shown on a 65-point geometric dome model created in STARMODAL

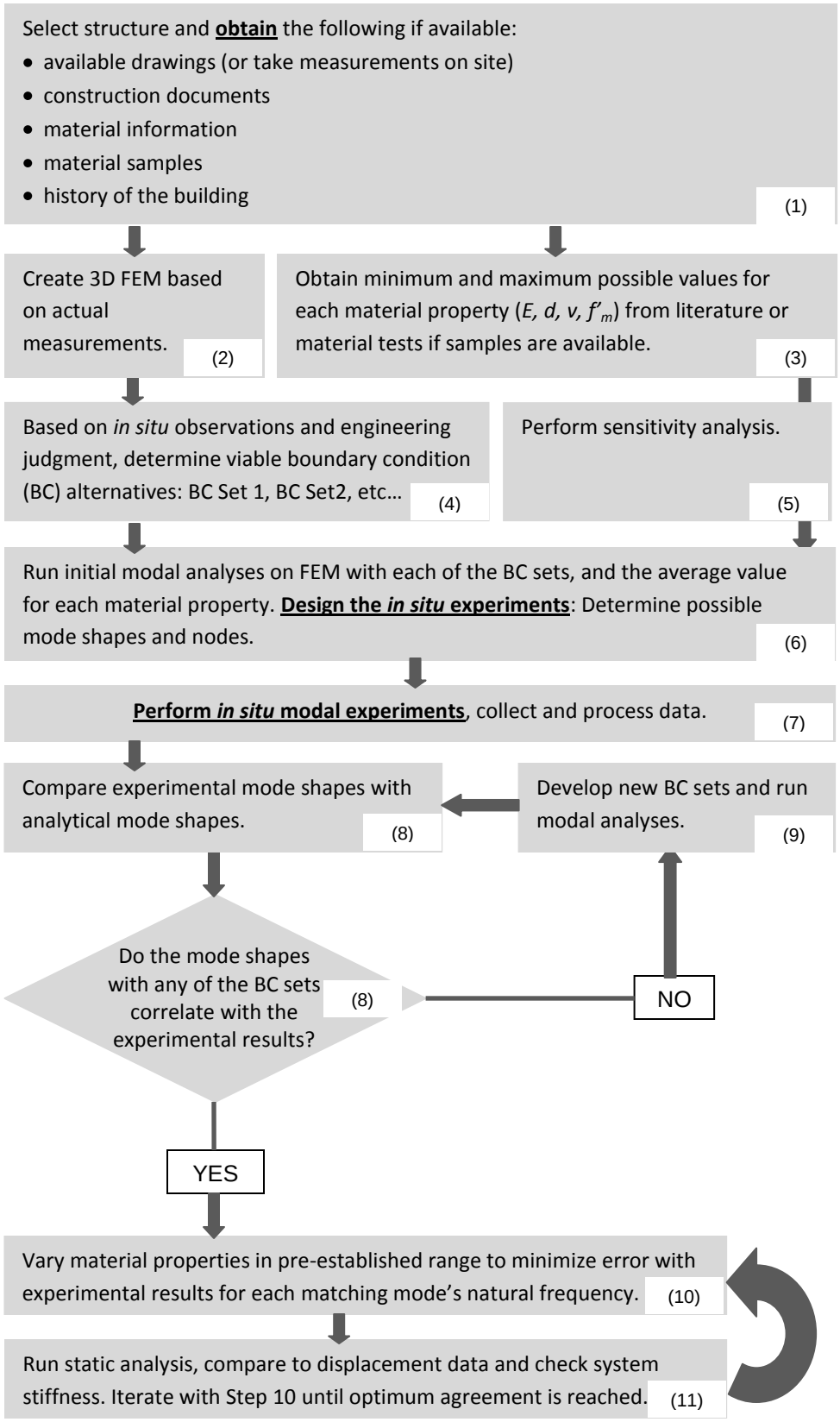

Figure 7. Summary of Experimental Modal Analysis Based FEM Updating Methodology

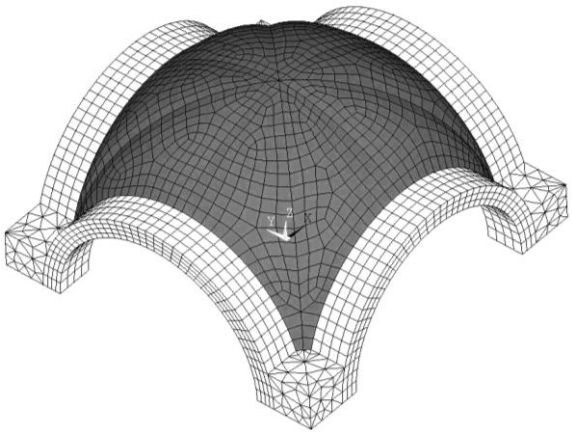

a) SHELL Dome Model

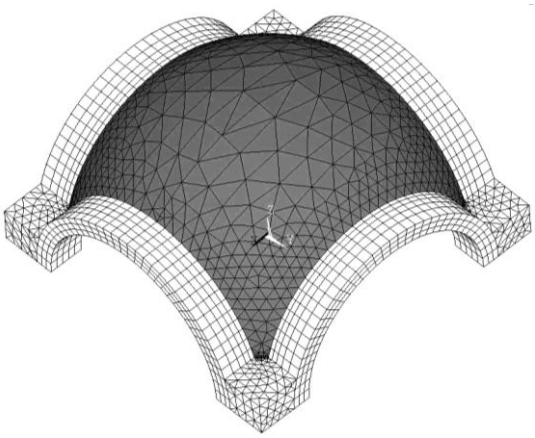

b) SOLID Dome Model

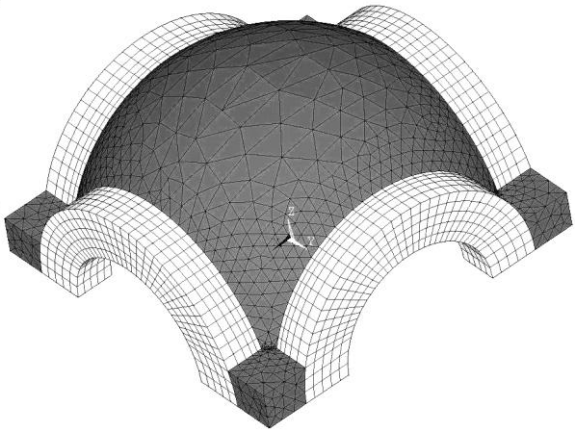

c) Hypothetical Thick Side Arch

Figure 8. Analytical Models for the *Model Dome*

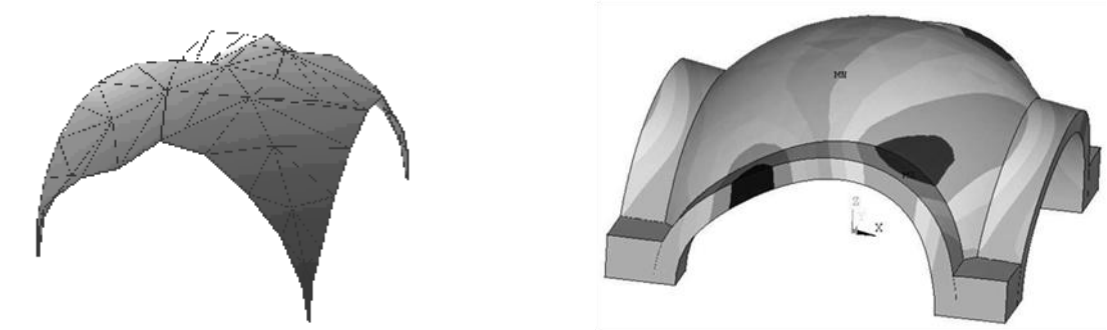

a) Experimental results b) Analytical results

Figure 9. Comparison of experimental and analytical mode shapes for Mode #1

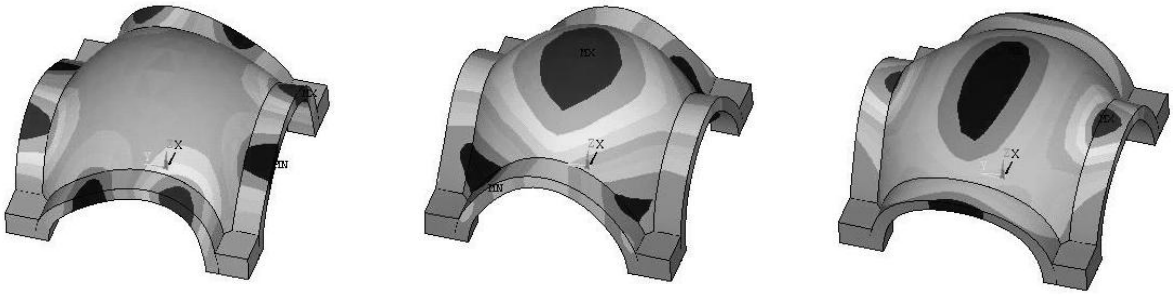

a) Deformed Shape for Mode 2 b) Deformed Shape for Mode 3 c) Deformed Shape for Mode 4

Figure 10. Analytical mode shapes for the SOLID model

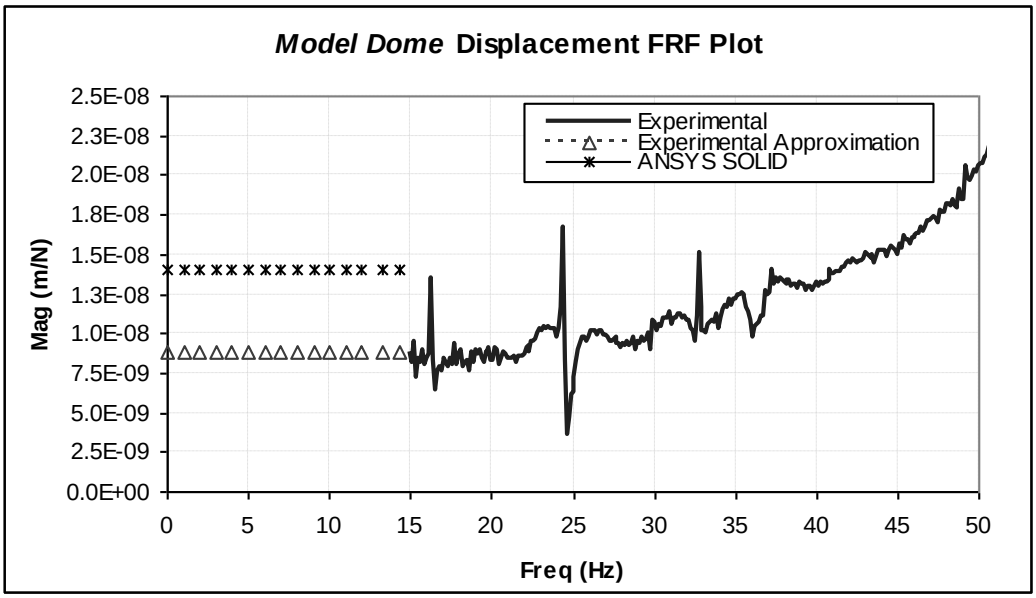

Figure 11. Frequency Response Function Displacement Magnitude Plot for one of the experiments conducted for the *Model Dome* and the comparison to the analytical approximation

Table 1. Model Dome Components and Materials

Element/Material	Actual Dome	Model Dome
Tiles for the dome webbing	Guastavino tiles 15 cm × 30 cm × 2.5 cm (6 in × 12 in × 1 in , *source: NE Capitol archive*)	Clay face brick units 10 cm × 20 cm x 1.25 cm (8 in. x 4 in. x ½-inch)
Side arches and piers	Indiana limestone blocks, approximately 46 cm thick (18 in) thick (Figure 1)	Regular clay brick units and Portland cement lime (PCL) mortar are used (Figure 2)
Mortar Mixture	First layer: Fast setting mortar (gypsum mortar) Top layers: Weatherproof Portland cement mortar	First layer: Plaster of Paris Top layers: Portland cement lime (PCL) mortar is anticipated

Table 2. Initial Material Property Ranges for *Model Dome* based on Laboratory Testing

	f'_m range from experiments	E_m range based on $E_m = 700f'_m$
Material Set 1: **Clay Brick + PCL Mortar**	9.65-15.86 MPa (1,400- 2,300 psi)	6.89-11.03 GPa (1,000- 1,600 ksi)
Material Set 2: **Clay Thin (Face) Brick + Plaster of Paris**	8.27-11.03 MPa (1,200- 1,600 psi)	6.21-7.93 GPa (900- 1,150 ksi)

Table 3. *Model Dome* Finite Element Models- Parametric Sensitivity Analysis Results

A. SOLID Model				B. SHELL Model			
Material Set 1: Clay brick + PCL Mortar				**Material Set 1: Clay brick + PCL Mortar**			
Parameter (1% Increase)	**Reference modes**	**% change in ω**	**Character**	**Parameter (1% Increase)**	**Reference modes**	**% change in ω**	**Character**
Modulus of Elasticity (E)	mode 1 (ω_1)	0.35%	increase	Modulus of Elasticity (E)	mode 1 (ω_1)	0.40%	increase
	mode 6 (ω_6)	0.23%	increase		mode 9 (ω_9)	0.17%	increase
Density (d)	mode 1 (ω_1)	0.31%	decrease	Density (d)	mode 1 (ω_1)	0.29%	decrease
	mode 6 (ω_6)	0.29%	decrease		mode 9 (ω_9)	0.16%	decrease
Possion's Ratio (v)	mode 1 (ω_1)	0.01%	increase	Possion's Ratio (v)	mode 1 (ω_1)	0.00%	increase
	mode 6 (ω_6)	0.00%	increase		mode 9 (ω_9)	0.00%	decrease
Material Set 2: Thin (face) brick + Plaster of Paris				**Material Set 2: Thin (face) brick + Plaster of Paris**			
Parameter (1% Increase)	**Reference modes**	**% change in ω**	**Character**	**Parameter (1% Increase)**	**Reference modes**	**% change in ω**	**Character**
Modulus of Elasticity (E)	mode 1 (ω_1)	0.13%	increase	Modulus of Elasticity (E)	mode 1 (ω_1)	0.08%	increase
	mode 6 (ω_6)	0.24%	increase		mode 9 (ω_9)	0.29%	increase
Density (d)	mode 1 (ω_1)	0.11%	decrease	Density (d)	mode 1 (ω_1)	0.15%	decrease
	mode 6 (ω_6)	0.16%	decrease		mode 9 (ω_9)	0.34%	decrease
Possion's Ratio (v)	mode 1 (ω_1)	0.01%	decrease	Possion's Ratio (v)	mode 1 (ω_1)	0.01%	decrease
	mode 6 (ω_6)	0.02%	decrease		mode 9 (ω_9)	0.00%	increase

Table 4. Experimental results for the Model Dome for Natural Frequency Validation

Experimental Results			Analytical Results						Experimental & Analytical
			SHELL Dome Model			SOLID Dome Model			
Experiment Definition	Mode	Frequency (Hz)	Mode	Frequency (Hz)	% Error with Exp. Values	Mode	Frequency (Hz)	% Error with Exp. Values	Mode Shape Definition
Experimental Setup #1 (Figure 5a)	1	43.5	1	42.5	2.30%	1	45.2	3.91%	Side arches deflect in one horizontal direction at a time. Dome crown is a node.
	2	50.6	3	49.8	1.58%	2	45.4	10.30%	Both side arches-deflecting at the same time. Dome crown is a node.
						3	55.6	9.88%	
	3	86.7	9	81.4	6.08%	6	83.4	3.82%	Uniform compression for the entire structure.
			10	82.2	5.18%				
			11	84.0	3.13%				
Experimental Setup #2 (Figure 5b)	4	96.8	N/A			11	105.4	8.89%	Both side arches and the dome are deformed. Substantial motion at the crown.

Table 5. Final Material Properties for the *Model Dome* Finite Element Models

	Modulus of Elasticity Final Value	**Poisson's Ratio**	**Density**
	GPa (ksi)	**N/A**	**kg/m^3 (Slug/in^3)**
Material Set 1: Clay brick + PCL Mortar	10.34 (1,500)	0.24	2,300 (0.0026)
Material Set 2: Clay Thin (face) brick + Plaster of Paris	6.89 (1,000)	0.20	1,800 (0.0020)

Table 6. Experimental Results for the Model Dome for Stiffness Validation

Physical Characteristic	Experimental Values	Analytical Values			
		SHELL Dome Model		SOLID Dome Model	
		Value	% Difference w. Exp.	Analytical Value	% Difference w. Exp.
Flexibility @ Dome Crown (m/N)	8.80E-09	1.80E-07	1945.45%	1.40E-08	59.09%
Stiffness @ Dome Crown (kN/m)	113,636	5,652	95.03%	71,429	37.14%